J Stat Phys (2009) 135: 751–761
DOI 10.1007/s10955-009-9759-4

Numerical Studies of a Two-dimensional Navier-Stokes System with New Boundary Conditions

N. Chernov

Received: 31 March 2009 / Accepted: 13 May 2009 / Published online: 27 May 2009

Abstract In this paper we describe the results of numerical studies of solutions of the Navier-Stokes System (NSS) under the boundary conditions introduced recently in the paper by Dinaburg et al. (A new boundary problem for the two-dimensional Navier-Stokes system, see this issue of this journal). First, we investigate the decay of Fourier modes, confirming the results and conjectures made in Dinaburg et al. (A new boundary problem for the two-dimensional Navier-Stokes system, see this issue of this journal). Second, we explore the growth of the total energy and enstrophy, which is possible under the adopted boundary conditions. We show that the solutions of the finite-dimensional Galerkin approximations to the NSS may diverge to infinity in finite time, i.e. their energy may blow up.

Keywords Navier-Stokes · Fluid dynamics · Blow-ups

1 Introduction

Dinaburg et al. [1] have recently studied the two-dimensional Navier-Stokes System (NSS)

$$\frac{\partial \omega}{\partial t} + u_1 \frac{\partial \omega}{\partial x} + u_2 \frac{\partial \omega}{\partial y} = \Delta \omega \tag{1}$$

for an incompressible fluid in a square

$$Q = [0, \pi] \times [0, \pi]$$

The author thanks Ya. Sinai and D. Li for involving him in this interesting work, N. Simanyi for help in the analysis of eigensolutions, and A. Korepanov for assistance with Mathematica-based computations. The author was partially supported by NSF grant DMS-0652896.

N. Chernov (✉)
Department of Mathematics, University of Alabama at Birmingham, Birmingham, AL 35294, USA
e-mail: chernov@math.uab.edu

under the following boundary conditions

$$\begin{aligned} &u_1(t,x,y)=0 \quad \text{for all } (x,y)\in\partial Q \text{ and all } t\ge 0,\\ &\omega|_{x=0}=\omega|_{x=\pi}=0, \qquad \frac{\partial}{\partial y}\omega\Big|_{y=0}=\frac{\partial}{\partial y}\omega\Big|_{y=\pi}=0. \end{aligned} \tag{2}$$

Here $\mathbf{u}=(u_1,u_2)$ denotes the velocity vector and

$$\omega(t,x,y)=\frac{\partial u_1(t,x,y)}{\partial y}-\frac{\partial u_2(t,x,y)}{\partial x}$$

the vorticity; the incompressibility means that

$$\frac{\partial u_1(t,x,y)}{\partial x}+\frac{\partial u_2(t,x,y)}{\partial y}=0. \tag{3}$$

They proved that, under suitable assumptions on the initial state $\mathbf{u}(0,x,y)$, see below, the NSS is locally well posed (i.e. its solutions exist and are unique), and they obtained quantitative estimates on the decay of the corresponding Fourier modes. In this paper we present numerical results that support the conclusions and conjectures made in [1] about the decay of Fourier modes.

Next we note that the boundary conditions (2) in general do not preserve energy, since the fluid may have non-zero total flux through the two horizontal sides of Q. We show that in fact the total energy and enstrophy may grow rather sharply. Moreover, the solutions of the finite-dimensional Galerkin approximations to the NSS may diverge to infinity in finite time, i.e., blow up. We find diverging solutions numerically and construct them theoretically. This may be surprising as the solutions of two-dimensional NSS on a torus or a whole plane are known to be globally well posed (see, for example, [3]). We refer the interested reader to [1, 2] and references therein.

This paper is organized as follows. In Sect. 2 we verify the decay rates of the Fourier modes. In Sect. 3 we explore the growth of energy of Galerkin solutions empirically, based on computer simulations. In Sect. 4 we construct blow-up Galerkin solutions theoretically. In Sect. 5 we summarize our results.

2 Rates of Decay of Fourier Modes

First we verify the quantitative estimates on the decay of Fourier modes obtained in [1]. The components u_1 and u_2 of the velocity vector are expanded into Fourier series as

$$u_1(t,x,y)=\sum_{m\ge1,n\ge1}\frac{h(t,m,n)}{m}\sin mx\sin ny$$

and

$$u_2(t,x,y)=\sum_{m\ge1,n\ge1}\frac{h(t,m,n)}{n}\cos mx\cos ny+\sum_{m\ge1}\frac{f(t,m)}{m}\cos mx,$$

where $h(t,m,n)$ and $f(t,m)$ are the modes characterizing the solution of the NSS. It was shown in [1] that if the initial state satisfies

$$\begin{aligned} |h(0,m,n)| &\le \frac{D_0}{m^\alpha n^\beta}\cdot\frac{mn}{m^2+n^2}, \quad \forall m,n\ge 1,\\ |f(0,m)| &\le \frac{D_0}{m^\alpha}, \quad \forall m\ge 1, \end{aligned} \tag{4}$$

for some $\alpha > 2$ and $2 < \beta < 3$ with a constant $D_0 > 0$, then the NSS has a unique solution on some interval $(0, T)$ satisfying

$$\begin{aligned} |h(t,m,n)| &\le \frac{D_1}{m^\alpha n^\beta}\cdot e^{-\frac{m}{2}t}\cdot\frac{mn}{m^2+n^2}, \quad \forall m,n\ge 1,\\ |f(t,m)| &\le \frac{D_1}{m^\alpha}\cdot e^{-\frac{m}{2}t}, \quad \forall m\ge 1, \end{aligned} \tag{5}$$

for all $0 < t < T$. Furthermore, if D_0 in (4) is sufficiently small, then the solution of the NSS is global, and the bounds in (5) hold for all $0 < t < \infty$. The estimates (5) show that the decay in m is exponential for every $t > 0$, but the decay in n can be power-like, with a constant power $\beta \in (2, 3)$. The authors of [1] conjectured that their estimates were close to optimal, i.e. solutions with the decay rates (5) should exist. (In fact, it was shown in [1] that the optimal decay in n is n^{-5}.)

To verify these conclusions, we have computed the Fourier modes $h(t,m,n)$ and $f(t,m)$ in a numerical experiment where the initial values were set to

$$\begin{aligned} h(0,m,n) &= \frac{D_0}{m^\alpha n^\beta}\cdot\frac{mn}{m^2+n^2}, \qquad \forall m,n\ge 1,\\ f(0,m) &= \frac{D_0}{m^\alpha}, \qquad \forall m\ge 1, \end{aligned} \tag{6}$$

with $\alpha = 2.5$ and $\beta = 2.5$ and some $D_0 > 0$, so that the assumptions (4) are valid. It is shown in [1] that the modes $h(t,m,n)$ and $f(t,m)$ satisfy the system of ODE:

$$\begin{cases} \frac{d}{dt}h(t,m,n) = -\frac{mn}{m^2+n^2}N(t,m,n) - (m^2+n^2)h(t,m,n),\\ \frac{d}{dt}f(t,m) = -N(t,m,0) - m^2 f(t,m), \end{cases} \tag{7}$$

where $N(t,m,n)$ for $m \ge 1$ and $n \ge 0$ are quadratic polynomials of $h(t,m',n')$ and $f(t,m')$ for $m', n' \ge 1$; more precisely

$$\begin{aligned} N(t,m,n) = &\sum_{m',n',m'',n'=1}^{\infty} a_{m,n,m',n',m'',n''}h(t,m',n')h(t,m'',n'')\\ &+ \sum_{m',n',m'',n'=1}^{\infty} b_{m,n,m',n',m''}h(t,m',n')f(t,m'') \end{aligned} \tag{8}$$

for some constants $a_{m,n,m',n',m'',n''}$ and $b_{m,n,m',n',m''}$ given by explicit formulas; see [1]. For our numerical studies, we restricted the indices m, n to a finite interval $1 \le m, n \le K$ (which is a Galerkin approximation to the infinite system (7)). Then we solved the resulting finite-dimensional system numerically by the classical Runge-Kutta method. To test the accuracy we have changed the Galerkin size parameter K and the time step Δt in the Runge-Kutta scheme several times to make sure that our results remained stable.

Table 1 Power-law decay rates of the Fourier modes: the decay in n is given by b_1, the decay in m is given by b_2 and b_3 (for $h(t,m,n)$ and $f(t,m)$, respectively)

t	$K=20$						$K=30$		
	$D_0=1$			$D_0=10$			$D_0=10$		
	b_1	b_2	b_3	b_1	b_2	b_3	b_1	b_2	b_3
0.00	3.1	3.1	2.5	3.1	3.1	2.5	3.2	3.2	2.5
0.01	4.3	4.3	3.7	3.2	4.1	3.8	3.5	5.5	5.2
0.02	4.6	5.4	4.9	3.3	5.0	5.1	3.6	7.8	8.0
0.03	4.8	6.6	6.1	3.3	6.1	6.5	3.6	10.3	10.4
0.04	4.9	7.7	7.4	3.3	7.3	7.7	3.6	12.4	12.6
0.05	4.9	8.8	8.6	3.3	8.7	8.9	3.6	14.2	14.2
0.06	5.0	9.9	10.0	3.4	10.0	10.1	3.6	15.7	15.8
0.07	5.1	10.9	11.6	3.4	10.9	11.2	3.6	16.4	16.7
0.08	5.1	11.8	12.5	3.4	10.9	11.6	3.6	16.3	16.6

After computing the Fourier modes $h(t,m,n)$ and $f(t,m)$ we estimated their decay rates in m and n by approximating their logarithms

$$\tilde{h} = \log|h(t,m,n)| \quad \text{and} \quad \tilde{f} = \log|f(t,m)|$$

by three linear functions:

$$\begin{aligned} \tilde{h} &= a_1 - b_1 n \quad (\text{when } m \text{ is kept fixed}),\\ \tilde{h} &= a_2 - b_2 m \quad (\text{when } n \text{ is kept fixed}),\\ \tilde{f} &= a_3 - b_3 m. \end{aligned}$$

The slopes b_1, b_2, and b_3 represent the powers of the decay rates of $h(t,m,n)$ and $f(t,m)$ in n and m, respectively. Since the value of b_1 depends on m and the value of b_2 depends on n, we averaged the values of b_1 over $m=1,2,3$ and averaged the values of b_2 over $n=1,2,3$.

Table 1 shows how the computed values of b_1, b_2, and b_3 change in time. We see that the decay rates in m (given by b_2 and b_3) increase steadily (we conjecture that it grows linearly in t), indicating that the true decay becomes faster than any power function, which is consistent with the exponential bound (5). On the other hand, the decay rate in n (the value of b_1) remains nearly unchanged. (We note that, according to (5), the correct decay in n, for small fixed m's, is $n^{-(\beta+1)}$, so in our case the minimal value of b_1 should be close to 3.5).

Our results support the conclusions and conjectures stated in [1]: the decay of the Fourier modes in m is indeed much faster than the decay in n. Actually, the former is faster than any power function, while the latter remains power-like.

The value of D_0 in our tests was set to 1 and 10, see Table 1. We found that for $D_0 \le 10$ the numerical values of the Fourier coefficients $h(t,m,n)$ and $f(t,m)$ decrease in time. The total energy computed by

$$\begin{aligned} E(t) &= \frac{1}{2}\int_0^\pi \int_0^\pi \big([u_1(t,x,y)]^2 + [u_2(t,x,y)]^2\big)\,dx\,dy \\ &= \frac{\pi^2}{8}\sum_{m,n\ge 1} h^2(t,m,n)\left(\frac{1}{m^2}+\frac{1}{n^2}\right) + \frac{\pi^2}{4}\sum_{m\ge 1}\frac{f^2(t,m)}{m^2} \end{aligned} \tag{9}$$

Table 2 Energy and enstrophy, as well as their derivatives, at $t = 0$, as functions of D_0; see (6)

D_0	Energy		Enstrophy	
	E	dE/dT	S	dS/dt
1	3.1	−7	3.9	−11
5	78.0	−124	97.1	−187
10	312.2	−215	388.5	−285
13	527.6	−75	656.6	−15
14	611.8	23	761.5	163
20	1248.7	1390	1554.0	2520
100	3×10^4	5×10^5	4×10^4	8×10^5
10^3	3×10^6	6×10^8	4×10^6	9×10^8
10^4	3×10^8	6×10^{11}	4×10^8	9×10^{11}
10^5	3×10^{10}	6×10^{14}	4×10^{10}	9×10^{15}

and the total enstrophy

$$S(t) = \int_0^\pi \int_0^\pi [\omega(t, x, y)]^2 \, dx \, dy$$
$$= \frac{\pi^2}{4} \sum_{m,n \geq 1} h^2(t, m, n) \left(\frac{m}{n} + \frac{n}{m} \right)^2 + \frac{\pi^2}{2} \sum_{m \geq 1} f^2(t, m) \tag{10}$$

also decrease in time indicating the existence of a global solution of the NSS, in accordance with the theoretical analysis of [1].

On the contrary, when the value of D_0 is large, the theorem proven in [1] only guarantees the existence and uniqueness of a solution on a finite interval of time. We show next that the Fourier modes, the total energy and enstrophy can grow, rather sharply, and the solutions of the Galerkin approximations can diverge to infinity in finite time.

3 Blow-up of Solutions

Table 2 shows the initial energy E and enstrophy S, as well as their initial derivatives dE/dt and dS/dt (all taken at the time $t = 0$) versus the value of D_0 in (6). (We note that the power-like decay of the initial modes in (6) guarantees the existence of the energy and enstrophy, as well as their derivatives, at time $t = 0$.) When $D_0 \leq 13$, the energy and enstrophy start decreasing right away, and keep decreasing as t grows. This indicates that the solutions remain bounded, and apparently we can set $D_1 = D_0$ in (5).

When $D_0 \geq 14$, the energy and enstrophy start increasing, and for large values of D_0 their rate of increase is sharp. This implies, at least, that D_1 in (5) must be much larger than D_0, but we also explored what this initial growths may lead to when one solves the NSS numerically, via Galerkin approximations. We found that solutions of the Galerkin system of ODE (7) may actually diverge, i.e. grow to infinity in finite time. We present numerical evidence of this phenomenon below, and in the next section we construct diverging solutions theoretically.

Figure 1 illustrates the evolution of the energy and enstrophy when $D_0 = 10^4$, on a logarithmic scale. The solid line is $\log[E(t)/E(0)]$ and the dotted line is $\log[S(t)/S(0)]$, both

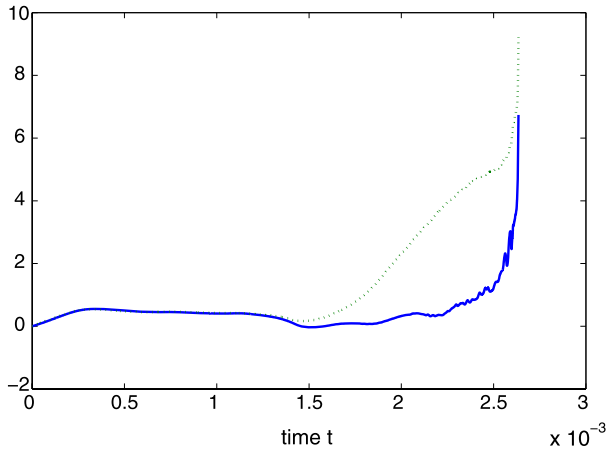

Fig. 1 The energy (*solid line*) and the enstrophy (*dotted line*), on the logarithmic scale, versus time

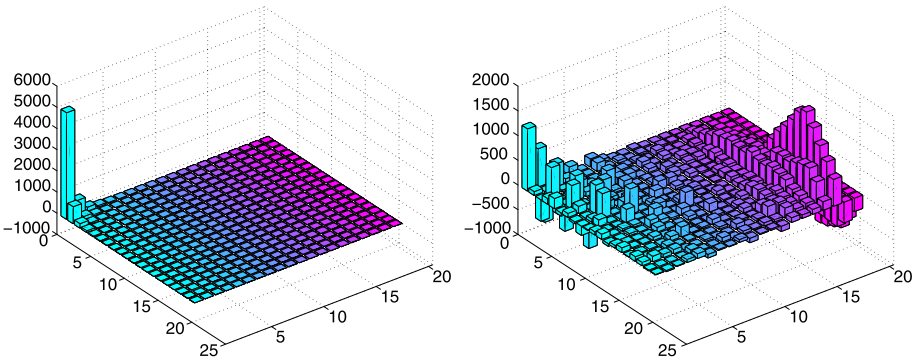

Fig. 2 The Fourier modes $h(t, m, n)$ for $0 \le m, n \le 20$, at time $t = 0$ (*left*) and at time $t = 0.0016$ (*right*). Note different vertical scaling (chosen automatically by MATLAB): the highest mode on the left is 5000 and the highest mode on the right is only 1200

versus time t. Initially, both logarithms are zeros, but then they grow, and in a short time they reach values of 7 and 9, respectively. Thus the energy has increased to $e^7 \sim 1000$ its initial value, and the enstrophy has increased to $e^9 \sim 10000$ its initial value (at this point we stopped the experiment to avoid numerical overflow).

Note that the growth of energy and enstrophy is not monotonic, the real uphill climb begins about half-way to the final point, at about $t = 0.0016$. During an initial quiescent period (in Fig. 1, it is $0 < t < 0.0016$) both functions remain nearly constant and even show a brief decline. Then the enstrophy starts moving up steadily, and when it reaches $e^4 \sim 50$ times its initial value, the energy begins its rapid increase, too. In the end, both functions rise sharply reaching a blow-up.

Figure 2 illustrates the distribution of the h-modes given by (6). The left panel of Fig. 2 shows the initial distribution, at time $t = 0$, where all the modes are positive and the large modes are tightly clumped near the corner $m = n = 1$ (far left in the picture). The right panel shows the mid-way distribution corresponding to $t = 0.0016$ (the time when the enstrophy just starts growing). By this time many negative modes have appeared and some large modes

have moved away from the left corner $m = n = 1$. The f-modes $f(t, m)$ (not shown in the figure) change similarly.

We see that during the initial period, when the total energy and enstrophy remain nearly constant, the Fourier coefficients $h(t, m, n)$ and $f(t, m)$ 'regroup': the values of $h(t, m, n)$ and $f(t, m)$ with larger indices m and n ('high modes') grow, while those with smaller indices ('low modes') decrease. By the end of the quiescent period, the dominant values of $h(t, m, n)$ and $f(t, m)$ move to the 'outer boundary' of the finite-size Galerkin area, i.e. the largest values of $h(t, m, n)$ and $f(t, m)$ are attained at $m, n \sim K$. After that the energy and enstrophy begin rapid grows and soon the solution blows up.

However, when large Fourier modes appear at the outer boundary of the finite-size Galerkin area, the Galerkin system ceases to be a good approximation to the real NSS, as its boundaries impose severe restrictions preventing further drift of the dominant Fourier modes. Thus the blow-up of our numerical solutions cannot imply a similar behavior of the real solutions of the NSS. Still we regard it as an interesting phenomenon, and we further investigate it theoretically in the next section.

4 Eigensolutions

The right hand side of the ODE system (7) is the sum of two parts: the first part involving $N(t, m, n)$ is a quadratic polynomial in Fourier modes $h(t, m, n)$ and $f(t, m)$, and the second part is linear in h's and f's. If a solution diverges to infinity, the quadratic part dominates, thus the linear part becomes negligible and can be discarded.

We note that the linear part in (7) comes from the Laplacian $\Delta\omega$ in the NSS (1), thus discarding it is equivalent to replacing the Navier-Stokes system (1) with the corresponding Euler equation

$$\frac{\partial \omega}{\partial t} + u_1 \frac{\partial \omega}{\partial x} + u_2 \frac{\partial \omega}{\partial y} = 0, \tag{11}$$

under the same boundary conditions (2) and the incompressibility assumption (3).

Now the ODE system for the Euler equation is obtained from (7) by the removal of its linear part; we rewrite it as

$$\frac{d}{dt} w_k(t) = \sum_{i,j \geq 1} q_{ijk} w_i(t) w_j(t) \quad \forall k \geq 1, \tag{12}$$

where $w_k(t)$ denote all the Fourier coefficients $h(t, m, n)$ and $f(t, m)$, numbered in an arbitrary order, and q_{ijk} is a 3D array of constant coefficients. Its finite-dimensional Galerkin approximation is

$$\frac{d}{dt} w_k(t) = \sum_{i,j=1}^{M} q_{ijk} w_i(t) w_j(t) \quad \forall k = 1, \ldots, M = K^2 + K, \tag{13}$$

which is a system of quadratic ODE's with constant coefficients. (Note that in a Galerkin approximation of size K to (7), there are K^2 modes $h(t, m, n)$ and K modes $f(t, m)$, hence there are a total of $M = K^2 + K$ modes.)

We will look for one-dimensional invariant subspaces of solutions of (13), i.e. solutions of the form

$$w_k(k) = g(t) v_k \quad \forall k = 1, \ldots, M, \tag{14}$$

where $g(t) = g_M(t)$ is a scalar function and v_k are some constants. Substituting this into (13) we obtain two equations:

$$\sum_{i,j=1}^{M} q_{ijk} v_i v_j = \lambda v_k \quad \forall k = 1, \dots, M \tag{15}$$

for some constant λ and

$$\frac{d}{dt} g(t) = \lambda g^2(t). \tag{16}$$

We say that $V = \{v_k\}$ is a 'tensor eigenvector' for the 3D tensor $\{q_{ijk}\}$ if it satisfies (15) with a constant λ (we call the latter a 'tensor eigenvalue'). The resulting solution (14) can be called an 'eigensolution'.

Note that if a pair (V, λ) satisfies (15), then so does $(cV, c\lambda)$ for any scalar c. Thus the one-dimensional 'tensor eigenspace' is well defined, but the 'tensor eigenvalue' is not. Precisely, there are two types of 'tensor eigenpairs': those with $\lambda = 0$, and those with $\lambda \neq 0$, in the latter case any scalar $\lambda \neq 0$ would be a 'tensor eigenvalue'.

The 'zero tensor eigenpairs' $(V, 0)$ give us stationary solutions to the Galerkin system (13), i.e. $w_k(t) = C v_k$, where C is a constant. Every 'non-zero tensor eigenpair' (V, λ), $\lambda \neq 0$, gives us a solution that blows up in finite time. Indeed, solving (16) we get

$$g(t) = \frac{g(0)}{1 - g(0)\lambda t}, \tag{17}$$

which diverges at time $t = [g(0)\lambda]^{-1}$ provided that $g(0)\lambda > 0$.

Now, interestingly, every 3D tensor has 'tensor eigenpairs':

Fact *For every 3D tensor $Q = \{q_{ijk}\}$, $1 \le i, j, k \le M$, there is a vector $V = \{v_k\}$ and a scalar λ satisfying* (15).

This fact might be known in algebra, but we could not locate a reference, so we provide a short proof.

Proof Given a vector $V = \{v_k\} \in \mathbb{R}^M$, denote by $V' \in \mathbb{R}^M$ the left hand side of (15). If there are no solutions to (15), then $V' \neq 0$, and the map $F: V \mapsto V'/\|V'\|$ transforms the sphere $\mathbb{S}^{M-1}$ into itself without fixed points. Clearly, the degree of F is an even number, because $F(-V) = F(V)$. On the other hand, $F(V)$ is never equal to $-V$ (otherwise $-V$ would be an eigenvector), hence there exists an arc of a great circle, shorter than π, that connects V with $F(V)$. Therefore F and the identity map are homotopic to each other, which implies that they share the same degree 1, a contradiction proving the Fact. □

Thus our system (13) always has eigensolutions. For example, since the terms $[f(t, m)]^2$ are missing in (8), every vector with exactly one non-zero w_k corresponding to an $f(t, m)$ (and all the other w_k's set to zero) would be a 'tensor eigenvector' with $\lambda = 0$. The corresponding solution would be stationary for the Euler equation (11). Our numerical tests reveal many stationary solutions of the Galerkin system (13), even for small K.

On the other hand, every non-zero 'tensor eigenpair' (V, λ), $\lambda \neq 0$, gives us a diverging solution. It will diverge faster when λ is larger, due to (17). We found that for some K (such as $K = 3, 5$) there are no 'tensor eigenpairs' (V, λ) with $\lambda \neq 0$, but for others such pairs

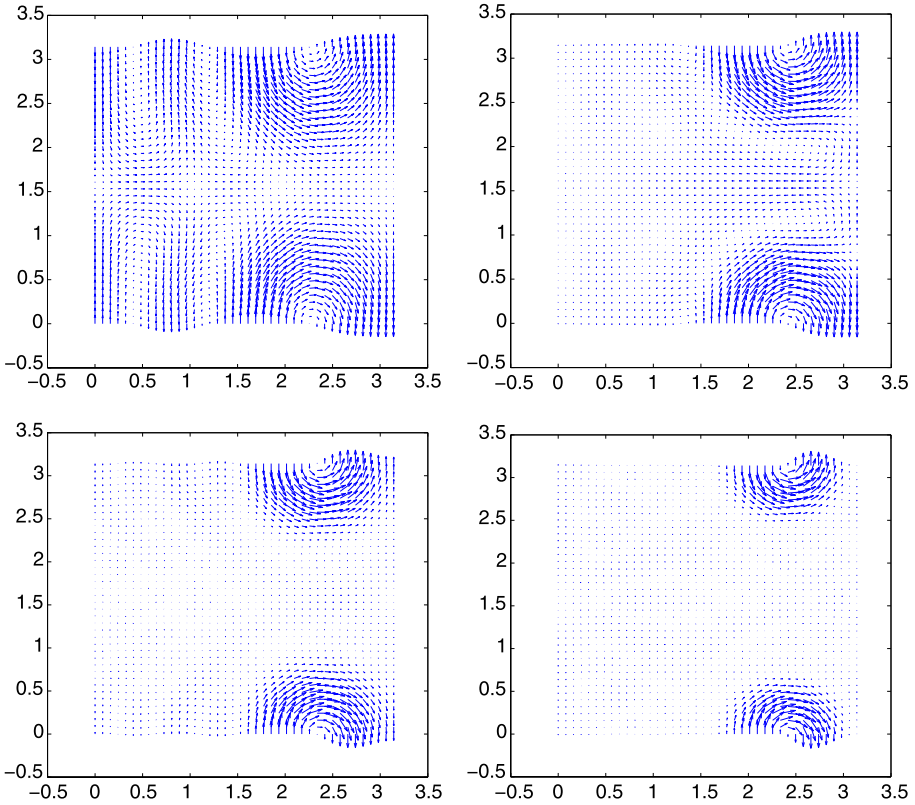

Fig. 3 The velocity portraits of the 'eigensolutions' corresponding to $K = 4$ (*top left*), $K = 6$ (*top right*), $K = 8$ (*bottom left*) and $K = 10$ (*bottom right*)

exist. In particular, they exist for $K = 4, 6, 8, \ldots, 20$. We conjecture that non-zero 'tensor eigenvalues' exist for all even $K \geq 4$. For example, for $K = 4$ there are 10 such solutions.

For $K = 4$, there is a 'tensor eigenpair' (V, λ) with $\lambda = 0.10$ (note that λ is not well defined, as it scales with V, so we computed λ when the vector V was normalized). The vector V corresponds to the solution shown in the top left panel of Fig. 3.

This solution belongs to a one-dimensional invariant space, hence the velocity portrait remains unchanged, i.e. all the vectors just grow by the same factor $g(t)$, as time goes on; in a finite time they all become infinite and the solution blows up. We emphasize that this is an analytic fact, not a computer simulation.

For $K = 6, 8, 10, \ldots$, there are similar 'tensor eigenpairs' (V, λ) with $\lambda > 0$, and the corresponding velocity portraits are shown in the three other panels of Fig. 3. They all produce diverging 'eigensolutions' for the corresponding Galerkin systems.

The solutions for different values of K in Fig. 3 have similar patterns, except for larger K's the swirls get more narrow and rotate faster, so that the rest of the velocity field is scaled down in the MATLAB-generated graphics images. The velocity portraits for larger values of K (from 12 to 20) remain very similar, indicating the existence of a limit as $K \to \infty$.

On the other hand, the corresponding eigenvalues get smaller as K grows (all the eigenvalues are computed when the eigenvectors are normalized). For example, we found $\lambda = 0.1024$ for $K = 4$, then $\lambda = 0.0082$ for $K = 10$, and $\lambda = 0.0003$ for $K = 20$. When

λ gets smaller, the divergence time increases, due to (17), thus in the limit $K \to \infty$ the divergence may evaporate, i.e. the limit solution may be defined for all $t < \infty$.

This concludes our numerical studies. Most of the computations were performed in MATLAB. The search for eigenvectors for $K = 3, 4, 5$ was also done in computer algebra system Mathematica by UAB graduate student A. Korepanov.

Symmetries One may notice that all the velocity portraits in Fig. 3 are symmetric with respect to the horizontal line $y = \pi/2$, the bottom half being a mirror image of the top half. This corresponds to one of the three natural symmetries in our problem.

Vertical symmetry:

$$u_1(t, x, y) = u_1(t, x, \pi - y)$$

and

$$u_2(t, x, y) = -u_2(t, x, \pi - y)$$

for all $x, y \in Q$ and $t \geq 0$. If this holds for $t = 0$, then it will hold for all $t > 0$. In this case more than half of the Fourier coefficients vanish: $h(m, n) = 0$ whenever n is even and $f(m) = 0$ for all m.

Horizontal symmetry:

$$u_1(t, x, y) = -u_1(t, \pi - x, y)$$

and

$$u_2(t, x, y) = u_2(t, \pi - x, y)$$

for all $x, y \in Q$ and $t \geq 0$. If this holds for $t = 0$, then it will hold for all $t > 0$. In this case half of the Fourier coefficients vanish: $h(m, n) = 0$ whenever m is odd and $f(m) = 0$ whenever m is odd.

Central symmetry:

$$u_1(t, x, y) = -u_1(t, \pi - x, \pi - y)$$

and

$$u_2(t, x, y) = -u_2(t, \pi - x, \pi - y)$$

for all $x, y \in Q$ and $t \geq 0$. If this holds for $t = 0$, then it will hold for all $t > 0$. In this case half of the Fourier coefficients vanish: $h(m, n) = 0$ whenever $m + n$ is even and $f(m) = 0$ whenever m is even.

Note that each type of symmetry is invariant, i.e. it persists with time. The most 'efficient' is the vertical symmetry as it eliminates more than half of the Fourier modes. Two other symmetries eliminate half of the Fourier modes.

The central symmetry is particularly interesting, as in this case the center $(\pi/2, \pi/2)$ is a fixed point of the velocity field. Due to the incompressibility (3), that fixed point can only be one of two types: either a saddle or a neutral focus.

We have simulated many solutions having the central symmetry in which the energy started growing to infinity, expecting that a strong swirl would appear at the center. However, this did not happen, the center was always a saddle. Even if initially the center was a focus, it smoothly bifurcated to a saddle as the solution evolved preparing for a rapid growth.

5 Conclusions

We have confirmed main results and conjectures made in the theoretical studies of the two-dimensional Navier-Stokes System with novel boundary conditions by Dinaburg et al; see [1]. In particular, we estimated the rates of the decay of the Fourier modes.

We also and investigated the behavior of solutions of the finite-dimensional Galerkin approximations depending on the total initial energy. We showed that those solutions may diverge to infinity in a finite time, in particular their energy and enstrophy may blow up. We have observed the blow-up phenomena in numerical simulations and constructed exploding solutions theoretically.

References

1. Dinaburg, E., Li, D., Sinai, Ya.G.: A new boundary problem for the two-dimensional Navier-Stokes system (see this issue of the journal)
2. Dinaburg, E., Li, D., Sinai, Ya.G.: Navier-Stokes system on the flat cylinder and unit square with slip boundary conditions (submitted)
3. Ladyzhenskaya, O.A.: The Mathematical Theory of Viscous Incompressible Flow. Gordon and Breach, New York (1969)